Protein Engineering vol.1 no.4 pp.313–318, 1987

Comparison of the solution and X-ray structures of barley serine proteinase inhibitor 2

G.Marius Clore[3], Angela M.Gronenborn, Michael N.G.James[2], Mogens Kjaer[1], Catherine A.McPhalen[2] and Fleming M.Poulsen[1,3]

Max-Planck Institut für Biochemie, D-8033 Martinsried bei München, FRG, [1]Department of Chemistry, The Carlsberg Laboratory, Gamle Carlsbergvej 10, DK-2500 Valby Copenhagen, Denmark, and [2]Medical Research Council of Canada, Group in Protein Structure and Function, Department of Biochemistry, The University of Alberta, Edmonton, Alberta, T6G 2H7, Canada

[3]Authors to whom reprint requests should be sent

A comparison of the solution n.m.r. structures of barley serine protease inhibitor 2 (BSPI-2) with the X-ray structures of both subtilisin complexed and native BSPI-2 is presented. It is shown that the n.m.r. and X-ray structures are very similar in terms of overall shape, size, polypeptide fold and secondary structure. The average atomic rms difference between the 11 restrained dynamics structures on the one hand and the two X-ray structures on the other is 1.9 ± 0.2 Å for the backbone atoms and 3.0 ± 0.3 Å for all atoms. The corresponding values for the restrained energy minimized mean dynamics structure are 1.5 and 2.4 Å, respectively

Key words: barley serine protease inhibitor / n.m.r. solution structure / X-ray structure

Introduction

In the preceding paper (Clore *et al.*, 1987a) we presented the determination of the solution conformation of the 64 residue proteolytic fragment (residues 20–83) of barley serine proteinase inhibitor 2 (BSPI-2 also known as chymotrypsin inhibitor 2, CI-2) on the basis of n.m.r. data using a combination of distance geometry and restrained molecular dynamics calculations. In this paper we present a detailed comparison of the structures derived in this manner with two X-ray structures of BPSI-2: one in the native state (McPhalen and James, 1987) and the other in a complex with subtilisin (McPhalen *et al.*, 1985a). Given that relatively few protein structures have been solved to date by n.m.r., such a comparison is essential to evaluate the reliability and limitations of the n.m.r. approach as a method of structure determination.

Materials and methods

All structural analyses and comparisons were carried out with the program XPLOR (A.T.Brünger, unpublished data) which is a vectorized version of the program CHARMM (Brooks *et al.*, 1983) especially adapted for restrained molecular dynamics and structure analysis.

The X-ray structures used in the comparisons are taken from McPhalen *et al.* (1985a) and McPhalen and James (1987). The native (free) X-ray structure of BSPI-2 was solved at 2.0 Å resolution with a crystallographic R factor of 0.198 (McPhalen and James, 1987). The X-ray structure of BSPI-2 in the complex with subtilisin Novo was solved at 2.1 Å with a crystallographic R factor of 0.193 (McPhalen *et al.*, 1985a). The root mean square (rms) error in the atomic coordinates of the two X-ray structures is ~0.3 Å.

Results and Discussion

The notation employed for the structurés obtained from the distance geometry and restrained molecular dynamics calcula-

Table I. Interproton distance deviations and radii of gyration[a]

Structure	Rms difference between calculated and target interproton distance restraints (Å)				Radii of gyration (Å)
	All	Interresidue		Intraresidue	
		Short range ($\|i-j\|<5$)	Long range ($\|i-j\|>5$)		
	(403)	(140)	(70)	(193)	
<RDDG>	0.11 ± 0.01	0.12 ± 0.01	0.11 ± 0.02	0.09 ± 0.01	10.96 ± 0.14
$(\overline{RDDG})$m	*0.09*	*0.11*	*0.07*	*0.09*	*10.98*
Xray(free)	0.56	0.69	0.68	0.37	11.27
Xray(bound)	0.47	0.54	0.63	0.33	11.27
Xray-RM(free)	0.15	0.16	0.17	0.13	11.18
Xray-RM(bound)	0.14	0.15	0.16	0.13	11.11

[a]The notation of the X-ray structures is as follows: Xray(free) and Xray(bound) are the structures of native (McPhalen and James, 1987) and subtilisin complexed (McPhalen *et al.*, 1985a) BSPI-2, respectively. Xray-RM(free) and Xray-RM(bound) are the restrained energy minimized structures derived from the original X-ray structures (see text). <RDDG> are the 11 final restrained dynamics structures and $(\overline{RDDG})$m is the restrained energy minimized mean structure derived from the <RDDG> structures (Clore *et al.*, 1987a). The rms difference (rmsd) between the calculated (r_{ij}) and target restraints is calculated with respect to the upper (r_{ij}^u) and lower (r_{ij}^l) limits such that

$$\text{rmsd} = \begin{cases} [(r_{ij}-r_{ij}^u)^2/n]^{1/2} & \text{, if } r_{ij} > r_{ij}^u \\ 0 & \text{, if } r_{ij}^l \le r_{ij} \le r_{ij}^u \\ [(r_{ij}-r_{ij}^l)^2/n]^{1/2} & \text{, if } r_{ij} < r_{ij}^l \end{cases}$$

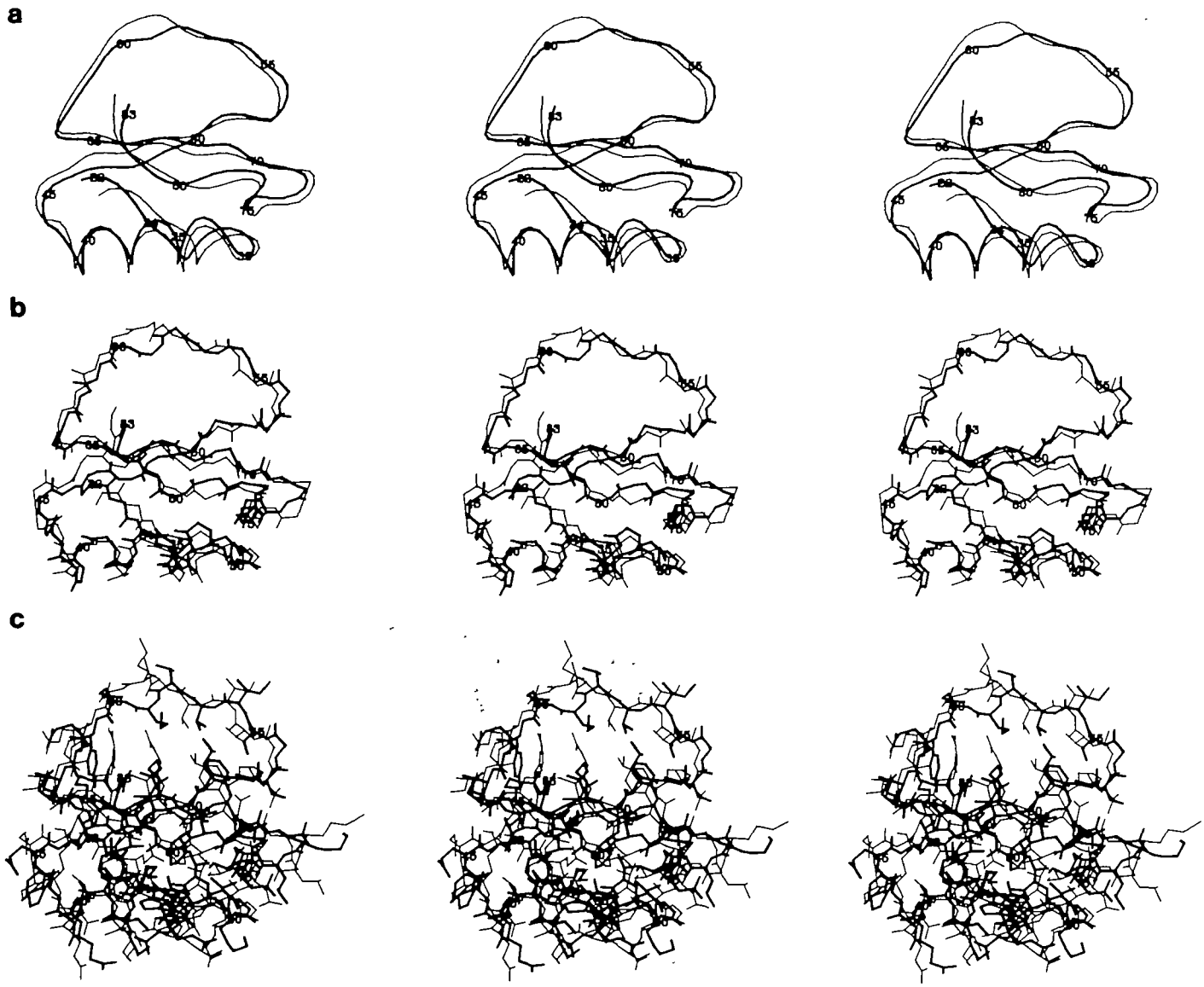

Fig. 1. Best fit superposition (residues 22–83) of the restrained energy minimized mean structure ($\overline{\text{RDDG}}$)m (thick lines) with the X-ray structure of native BSPI-2 (thin lines). (**a**) smoothed backbone (C,C^{α},N) atom representation; (**b**) backbone (C,C^{α},N,O) atoms; and (**c**) all atoms with the exception of hydrogens.

tions is the same as that in the previous paper (Clore *et al.*, 1987a) and for the sake of clarity will be briefly reiterated here; <DG> are the 11 converged distance geometry structures, <DGm> the structures derived from the <DG> structures by restrained energy minimization, and <RDDG> the structures derived from the <DGm> structures by restrained molecular dynamics; $\overline{\text{DG}}$, $\overline{\text{DGM}}$ and $\overline{\text{RDDG}}$ are the mean structures obtained by averaging the coordinates of the <DG>, <DGm> and <RDDG> structures best fitted to residues 22–83, and ($\overline{\text{DG}}$)m, ($\overline{\text{DGm}}$)m and ($\overline{\text{RDDG}}$)m are the structures derived from the mean structures by restrained energy minimization. In comparing these structures with the two crystal structures of BSPI-2 two points have to be considered: namely to what extent are the differences due (i) to the inadequacies of the n.m.r. data and (ii) to genuine differences between the solution and crystal structures. The inadequacies of the n.m.r. data are reflected by the limitations in the number and accuracy of the interproton distance and ϕ backbone torsion angle restraints as well as in the limited range (≤ 5 Å) of the interproton distance restraints.

Genuine differences between the solution and X-ray structures can be ascertained by comparing the values of the experimental n.m.r. restraints with an equivalent set derived from the X-ray structures. Such a comparison is afforded by the data in Tables I to III relating to the interproton distance restraints. The X-ray structures exhibit relatively large deviations with respect to the interproton distance restraints when compared to the restrained dynamics structures (Table I). This is also reflected by an approximately 60-fold higher value in the nuclear Overhauser enhancement (NOE) restraints energy (Table III). Table II details those interproton distances for which the X-ray structures exhibit violations >0.5 Å. This comprises 17 short ($|i-j| \leq 5$) and 10 long ($|i-j| > 5$) range interresidue distances and 12 intraresidue distances out of a total of 403 interproton distance restraints. These distance violations are distributed throughout the structure and the maximum violation is 4.8 Å. Thus it would appear that there are a few genuine differences between the X-ray and solution structures. We note, however, that the X-ray structures do not exhibit any significant deviations from the ϕ

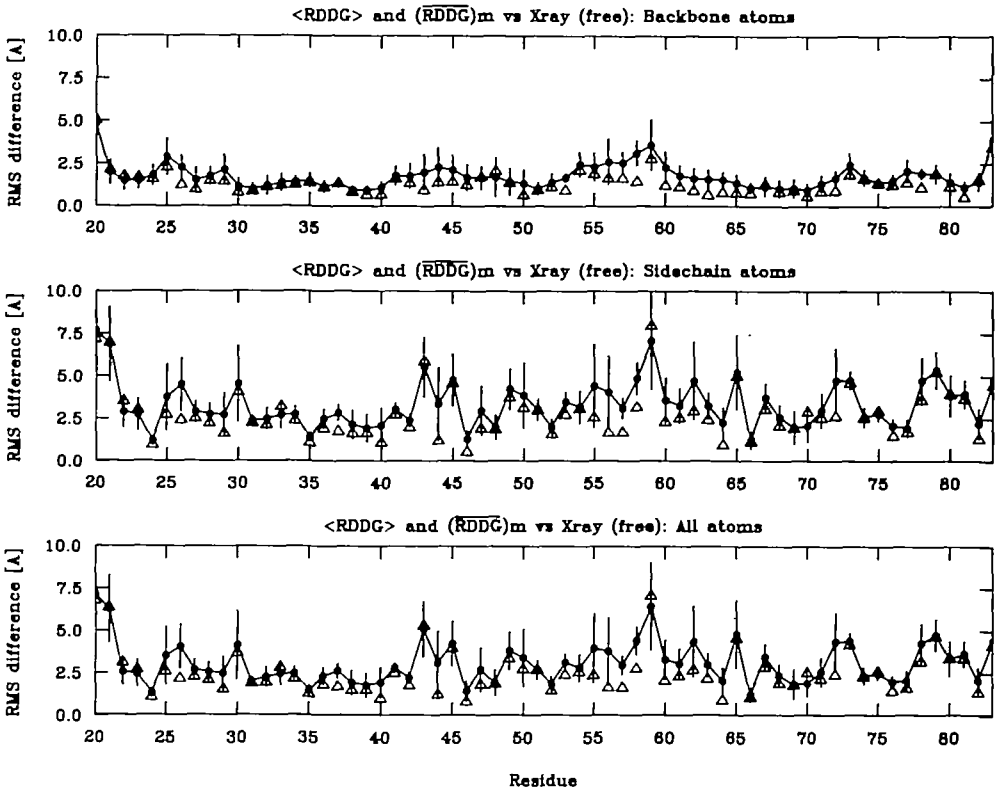

Fig. 2. Atomic rms difference between the <RDDG> (●) and (RDDG)m (△) structures on the one hand and the X-ray structure of native BSPI-2 on the other. The closed circles represent the average rms difference between the <RDDG> structures and the X-ray structure at each residue and the bars represent the standard deviations in these values.

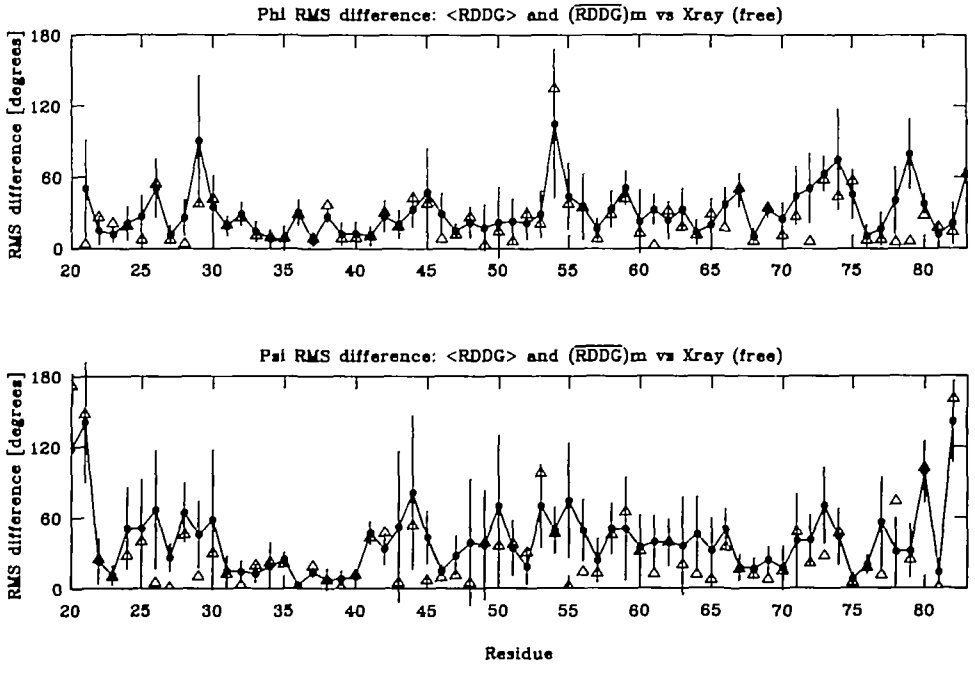

Fig. 3. ϕ and ψ angular rms differences between the <RDDG> (●) and (RDDG)m (△) structures on the one hand and the X-ray structure of native BSPI-2 on the other. The closed circles represent the average angular rms difference between the <RDDG> structures and the X-ray structure at each residue and the bars represent the standard deviations in these values.

backbone torsion angle limits derived from the $^3J_{HN\alpha}$ coupling constant data, as indicated by the low values of the ϕ restraints energy (Table III). To assess the structural significance of the interproton distance violations, we proceeded to test whether they could be partially remedied by only minor atomic rms shifts. We therefore subjected both crystal structures to restrained energy

Table II. Differences between the experimentally derived interproton distance restraints and the interproton distances derived from the X-ray structures of BSPI-2

Observed NOE	Observed NOE intensity[a]	Xray(free)/(bound)		Xray-RM(free/bound)	
		r_{ij}(Å)	Δ(Å)[b]	r_{ij}(Å)	Δ(Å)[b]
Short range ($\|i-j\| \leq 5$) interresidue					
V32HN-A35HB	m	5.3/5.5	1.5/1.7	4.4/4.4	0.6/0.6
E34HA-K37HN	m	4.0/3.8	0.7/0.5	3.3/3.3	0.0/0.0
E43HA-V38HN	m	4.8/4.7	1.5/1.4	3.7/3.7	0.4/0.4
A35HA-V38HG	m	4.6/4.6	0.8/0.8	2.7/3.9	0.0/0.1
K37HB-V38HA	m	4.6/4.1	1.3/1.1	3.5/3.6	0.2/0.3
I39HN-Q41HN	m	4.1/4.0	0.8/0.7	3.6/3.6	0.3/0.3
L40HB-D42HN	m	5.5/5.5	2.2/2.2	4.0/4.0	0.7/0.7
I49HD-L51HA	m	8.6/4.6	4.8/0.8	4.5/4.0	0.8/0.2
Y61HD-I63HA	m	5.6/5.0	2.3/1.7	3.7/3.6	0.4/0.3
Y61HE-I63HA	m	4.3/3.8	1.0/0.5	2.3/2.3	0.0/0.0
V66HG-R67HA	m	5.4/5.4	1.6/1.6	4.1/4.1	0.3/0.3
L68HA-F69HB	m	4.8/5.0	1.6/1.7	3.8/3.8	0.5/0.5
F69HD-V70HN	m	4.5/4.8	1.3/1.5	3.9/3.9	0.6/0.6
V70HG-D71HA	s	5.5/5.3	2.3/2.1	3.1/3.1	0.0/0.0
D71HN-I76HN	m	4.3/4.4	1.0/1.1	3.5/3.6	0.2/0.3
L73HN-D74HN	m	4.5/4.5	1.2/1.2	1.9/1.8	0.0/0.0
L76HA-A77HB	m	4.6/4.8	0.8/1.0	4.0/4.0	0.2/0.2
Long range ($\|i-j\| \leq 5$) interresidue					
E23HA-V82HN	m	4.0/3.9	0.7/0.6	3.5/3.5	0.2/0.2
W24HZ3-V66HG	s	3.8/3.6	0.6/0.4	3.4/3.4	0.2/0.2
W24HE3-P80HA	m	4.8/4.6	1.5/1.3	3.8/3.8	0.5/0.5
V32HA-L68HD	m	3.8/4.5	0.0/0.6	3.6/3.8	0.0/0.0
V32HN-V75HN	m	5.7/5.3	2.4/2.0	4.1/4.1	0.8/0.8
V32HN-N75HB	m	6.4/6.1	3.1/2.8	3.7/3.7	0.4/0.4
I39HN-A46HB	m	5.1/5.1	1.3/1.3	3.8/3.8	0.0/0.0
L51HD-F69HD	m	6.0/5.4	2.2/1.6	4.2/4.2	0.4/0.4
V57HG-F69HE	s	4.6/3.3	1.4/0.1	3.4/3.3	0.2/0.1
D71HN-A77HN	m	4.2/4.1	0.9/0.8	3.5/3.5	0.2/0.2
Intraresidue					
E26: HA-HG	m	3.9/3.9	0.6/0.6	3.6/3.6	0.3/0.3
I39: HN-HGm	m	4.6/4.6	0.8/0.8	4.0/4.0	0.2/0.2
HA-HD	m	4.7/4.7	0.9/0.9	4.2/4.2	0 4/0.4
I48: HN-HGm	m	4.6/4.6	0.8/0.8	4.1/4.1	0.3/0.3
HN-HD	m	4.4/4.2	0.6/0.4	3.9/3.8	0.1/0.0
I49: HA-HG	s	3.1/3.9	0.0/0.7	3.3/2.5	0.1/0.0
V50: HN-HG	s	4.5/4.6	1.3/1.4	3.3/3.4	0.1/0.2
T58: HN-HG	s	4.5/2.6	1.3/0.0	3.2/2.7	0.0/0.0
R62: HA-HG	m	2.7/4.5	0.0/1.2	2.8/2.2	0.0/0.0
I63: HA-HD	m	4.7/4.5	0.9/0.7	4.1/4.1	0.3/0.3
I68: HN-HD	m	4.4/4.6	0.6/0.8	3.9/4.0	0.1/0.2
I76: HN-HGm	s	4.6/4.6	1.4/1.4	3.5/3.5	0.3/0.3

[a]The NOE intensities are classified into strong (s), medium (m) and weak(w), and are taken to correspond to distance ranges of 1.8−2.7 Å, 1.8−3.3 Å and 1.8−5.0 Å, respectively. In the case of NOEs involving a methyl group(s), an additional 0.5 Å per methyl group is added to the upper distance limit to account for the higher intensity of methyl resonances.
[b]Δ represent the differences between the upper distance limits deduced from the experimental measurements on the one hand and the distances in the X-ray and restrained energy minimized X-ray structures on the other.

minimization using the same procedures as described in the previous paper (Clore *et al.*, 1987a). In both cases this resulted in small atomic rms shifts (<0.4 Å for all atoms; Table IV), significant improvements in the interproton distance deviations (Table I), violations (Table II) and NOE restraints energy (Table III), and a small reduction in the overall non-bonding energy (Table III). Indeed the values of the various parameters relating to the interproton distance restraints are comparable to those of the <DGm> structures (see Tables III and IV of Clore *et al.*, 1987a) but not quite as good as those of the <RDDG> structures. Thus in structural terms the differences between the structure in solution and the crystal structures must be relatively minor. It should also be noted in this respect that restrained energy minimization did not result in structural convergence as the atomic rms differences between the two restrained energy minimized X-ray structures is the same as that between the original X-ray structures themselves (Table IV).

The best-fit superpositions of the restrained energy minimized mean structure ($\overline{\text{RDDG}}$)m and the native X-ray structure illustrated in Figure 1 clearly shows the striking similarity of the two structures with respect to overall shape, size, polypeptide fold and secondary structure. The atomic and angular rms differences between the <DG>, <DGm> and <RDDG> structures on the one hand, and the X-ray and restrained energy minimized X-ray structures on the other are given in Tables IV and V, respectively, and a comparison of the backbone hydrogen bonds is given in Table VI. The <RDDG> structures are slightly closer on average to the X-ray structures than are either the <DG> or <DGm> structures both with respect to atomic rms differences (Table IV) and differences in backbone torsion angles (Table V). The latter are principally manifested by a reduction in the number of ϕ,ψ torsion angles deviating by more than 90° from their corresponding values in the X-ray structures. More interesting is the observation that the average structures are closer to the X-ray structures than any of the individual structures, and that the average restrained dynamics structure $\overline{\text{RDDG}}$ is significantly closer than either of the two other average structures (Table IV). This relationship is also preserved when the average structures are subjected to restrained energy minimization to produce structures that are reasonable stereochemically and energetically, despite that fact that this procedure results in atomic rms shifts of 0.6−0.7 Å for the backbone atoms. Thus, the atomic rms differences between the restrained energy minimized mean structure ($\overline{\text{RDDG}}$)m and the two X-ray structures is ~1.5 Å for the backbone atoms and ~2.3 Å for all atoms (Table IV), and the average ϕ,ψ angular rms difference is ~22° with only one ϕ and two ψ angles deviating by more than 90° (Table V). These findings mirror those that were found in our previous model calculations on crambin (Clore *et al.*, 1986b, 1987b; Brünger *et al.*, 1986).

Plots of the atomic and angular rms differences between the <RDDG> and ($\overline{\text{RDDG}}$)m structures on the one hand and the native X-ray structure on the other are shown in Figures 2 and 3. The largest differences, both for the backbone and sidechain atoms, are seen in the reactive site loop region (residues 54−61). This is perhaps not too surprising given that this region is less well determined than the rest of the protein (see Figures 2 and 3 of Clore *et al.*, 1987a) due to the presence of relatively few long range ($|i-j|>5$) restraints with which to orientate it relative to the main body of the molecule. Further, most of its sidechains are directed outwards from the surface of the protein and are relatively unconstrained by the experimental interproton distances. The largest differences between the two X-ray structures also occur in this region and are correlated with above average values for the temperature factors in the native BSPI-2 structure (McPhalen and James, 1987). The segments of closest agreement, on the other hand, occur in the regular secondary structure elements, namely the α-helix and the mixed parallel/antiparallel β-sheet. This is also reflected by a set of similar back-

Table III. Energies of the structures[a]

Structure	Energy (kcal/mol)										
	Total	Potential	Bond (1069)	Angle (1961)	Dihedral (528)	Improper (265)	van der Waals	Electrostatic	H-bond	NOE restraints[b] (403)	ϕ torsion restraints[b] (34)
Xray(free)	5031	−10	75	339	415	0.37	−224	−551	−63	5041	1
Xray(bound)	3509	−79	75	313	404	0.27	−287	−516	−68	3580	7
Xray-RM(free)	99	−246	89	420	359	0.11	−205	−827	−83	339	6
Xray-RM(bound)	52	−275	88	399	359	0.12	−216	−824	−81	324	3
<RDDG>	− 107 ± 116	−360 ± 91	81 ± 11	478 ± 48	326 ± 14	0.1 ± 0.02	−145 ± 26	−1040 ± 50	−61 ± 6	184 ± 26	9 ± 5
$\overline{\text{RDDG}}$m	228	81	82	502	407	0.2	−85	−767	−59	142	5

[a]The notation of the structures is the same as that in Table I. The total energy is the sum of the potential and restraints (NOE and ϕ) energies, and the potential energy is made up of all the other bonded and non-bonded energy terms. The number of terms for the bond, angle dihedral and improper dihedral (planarity) potentials and for the effective NOE interproton distance and ϕ backbone torsion angle restraints potential is given in parentheses.
[b]The NOE and ϕ torsion angle restraints force constants (cf Eq. 1 of Clore *et al.*, 1986b) have values of 40 kcal/mol/Å^2 and 80 kcal/mol/radian^2 respectively.

Table IV. Atomic rms differences between the solution and X-ray structures of BSPI-2[a]

Structure	Atomic rms differences (Å) for residues 22-83[b]			
	Backbone atoms		All atoms	
	Xray(free)/ Xray(bound)	Xray-RM(free)/ Xray-RM(bound)	Xray(free)/ Xray(bound)	Xray-RM(free)/ Xray-RM(bound)
<DG>	2 1 ± 0.17/ 2.13 ± 0.17	2.01 ± 0.17/ 2.12 ± 0.17	3.22 ± 0.21/ 3.29 ± 0.22	3 21 ± 0.20/ 3.28 ± 0.22
<DGm>	2.05 ± 0 16/ 2.08 ± 0.16	2.00 ± 0.16 2.10 ± 0 18	3.18 ± 0.19/ 3.25 ± 0.21	3.15 ± 0.19 3.23 ± 0.21
<RDDG>	1.94 ± 0.22/ 1 94 ± 0.22	1.81 ± 0.24/ 1 80 ± 0.25	3.00 ± 0.29/ 3.03 ± 0.30	2.89 ± 0.30/ 2.91 ± 0.29
$\overline{\text{DG}}$	1.85/1.89	1 81/1.88	2.71/2.79	2.70/2.79
$\overline{\text{DGm}}$	1.81/1.86	1.75/1.83	2.68/2.76	2.66/2.74
$\overline{\text{RDDG}}$	1.39/1.38	1.27/1.26	2.26/2.29	2.16/2.16
($\overline{\text{DG}}$)m	1.90/1.94	1.85/1.91	2.94/3 05	2.92/3.03
($\overline{\text{DGm}}$)m	1.87/1.91	1.80/1.87	2.88/3.00	2.86/2.98
($\overline{\text{RDDG}}$)m	1.49/1.49	1 28/1.26	2 37/2.44	2.29/2.30
Xray(bound)	0.45/ −	0.53/0.31	1.04/ −	1.06/0.33
Xray-RM(free)	0.35/0.53	− /0.45	0.38/1.06	− /1.02
Xray-RM(bound)	0.54/0.31	0.45/ −	1.07/0.33	1.02/ −

[a]The notation of the X-ray structures is the same as that in Table I. The notation of the n.m.r. structures is given in the text.
[b]The reason that residues 20 and 21 are excluded from the atomic rms differences is that their conformation could not be determined as no NOEs involving these two residues were observed.

Table V. ϕ,ψ angular rms differences and violations between the converged restrained dynamics structures <RDDG> and the restrained energy minimized average structures ($\overline{\text{DG}}$)m, ($\overline{\text{DGm}}$)m and ($\overline{\text{RDDG}}$)m structures on the one hand and the X-ray structures on the other

Structure	Xray(free)/Xray(bound)			
	rmsd_ϕ(°)	viol_ϕ	rmsd_ψ(°)	viol_ψ
<DG>	32 ± 19/32 ± 19	9/8	36 ± 19/36 ± 19	5/5
<DGm>	38 ± 16/28 ± 17	5/5	38 ± 20/38 ± 22	3/2
<RDDG>	29 ± 17/29 ± 17	2/2	35 ± 19/35 ± 19	2/2
($\overline{\text{DG}}$)m	25 ± 20/25 ± 23	3/3	20 ± 18/20 ± 18	8/8
($\overline{\text{DGm}}$)m	25 ± 21/28 ± 23	3/3	25 ± 21/24 ± 21	7/7
($\overline{\text{RDDG}}$)m	22 ± 16/21 ± 17	1/1	23 ± 18/23 ± 17	3/3
Xray(free) vs Xray(bound)	7.9 ± 8.0	0	7.1 ± 6.7	0

The angular violations are defined as the number of angles for which the average angular rms difference between the structures is greater than 90°; these angles are not included in the calculation of the average angular rms difference. The notation for the structures is the same as that in Tables I and III.

bone hydrogen bonds (Table VI).

The sidechain conformations, as expected, are less well determined by the n.m.r. data than the backbone conformation, with the result that the sidechain atomic rms differences between the computed structures and the X-ray structures are larger than those for the backbone atoms (Table IV). Nevertheless, the positions of sidechains within the protein interior are relatively well determined (Figures 1c and 2), while those at the surface which are not restrained by a dense network of interproton distance restraints tend to be poorly determined (e.g. in the reactive site loop). It is important to stress in this respect that, with the exception of the densely packed hydrophobic core where steric packing requirements come into play, the positioning of the sidechains depends entirely on the presence or absence of restraints. Thus, for example, the salt bridges between Arg 65 and Arg 67 on the one hand and residues of the reactive site loop on the other, which are characteristic not only of BPSI-2 but also of the structurally related protein eglin (McPhalen *et al.*, 1985b; Bode *et al.*, 1986) and which have been postulated to stabilize the conformation and orientation of the reactive site loop, are not present in any of the three restrained energy minimized mean structures. Given that the position and conformation of the loop is still relatively well determined from the n.m.r. data, one might be misled into thinking that these salt bridges do not play a major role in stabilizing the reactive site loop conformation in solution. Such an interpretation, however, is unwarranted. The orientation of the reactive site loop in the n.m.r. structures is in fact determined by the presence of NOEs bridging the hinges of the loop connecting it to the main body of the protein (see Figure 2c of Clore *et al.*, 1987a). These NOEs do not involve either Arg 65 or Arg 67. Consequently, the stabilizing salt bridges are not reproduced. The absence of detectable NOEs from the guanidinium group of these two residues to loop residues, which could have positioned these side chains appropriately, may be due to the large linewidths associated with the resonances of the exchangeable protons within the guanidinium group.

Table VI. Backbone hydrogen bonds in the restrained energy mean structures and the X-ray structures of BSPI-2[a]

D_i(N)-A_j(O)	$d_{N,O}$(Å) / A(N−H−O) (°)				
	(DG)m	(DGm)m	(RDDG)m	Xray(free)	Xray(bound)
Short range ($\|i-j\| \leq 5$)					
26,24			2.5/122		
27,24	3.0/152	3.1/152			
28,25					3.4/160
29,27		2.8/153			
30,27			2.8/176	3.1/161	2.8/151
30,28					3.4/123
35,31	2.6/150	2.6/153	2.6/164	2.8/164	2.9/163
36,32		3.2/140	3.2/139		
37,33	2.8/159	2.7/169	2.9/172		
37,34					3.2/125
38,34	2.6/152	2.7/158	2.7/170	3.3/142	3.3/161
39,35				3.1/171	3.0/174
39,36		2.8/121	3.0/130		
40,36	2.7/164	2.9/168	3.2/167	2.8/163	3.0/167
41,37	2.4/123	2.5/126	2.7/154		3.2/137
41,38				3.0/122	3.1/122
42,38				3.1/158	3.0/145
42,39			3.4/128		
43,39	2.7/152	2.8/157	2.5/142	2.6/136	2.6/156
46,43			3.3/148	2.9/162	3.0/158
48,46	2.8/141	2.7/141			
54,52			2.6/149		
55,52				3.4/138	
57,55	3.0/149	3.0/149			
60,58				2.6/140	
63,61			3.1/144		
65,62	31./161	2.9/161	2.7/161	3.1/157	3.3/159
71,75	3.0/168	3.0/166	2.8/176	3.1/158	3.1/163
74,71			3.3/148	2.9/157	3.0/165
75,73	2.4/121				
Number	13	15	18	16	18
Long range ($\|i-j\| > 5$)					
24,80	2.5/128	2.6/137	2.7/167	2.9/163	3.0/155
29,76				2.6/160	2.9/166
32,74	3.3/125	3.2/126	3.1/141		3.0/136
47,64				2.6/153	2.7/160
49,66	3.1/166		3.1/177	2.9/172	3.1/163
51,68	2.7/157	2.7/165	3.0/147	2.8/165	2.8/172
53,70	2.9/158	3.0/147	2.8/171	3.0/151	2.9/154
66,47			3.2/153	2.8/162	3.0/166
68,49	2.6/145	2.6/131	2.7/171	2.5/168	2.8/170
70,51	3.2/167			2.8/156	2.9/159
76,30	3.1/156	2.9/157	2.7/155	2.8/159	2.7/160
77,69			2.9/152	2.8/162	2.7/173
78,69			2.7/137		
82,22	2.6/120	2.7/161	2.8/159		
83,65				3.0/158	3.0/164
Number	9	7	11	13	14

The criteria for assigning backbone hydrogen bonds are as follows: $d_{N,O} \leq 3.3$ Å and $120° < A(N-H-O) \leq 180°$. The notation of the structures is the same as that in Table I and III.

Acknowledgements

This work was supported by the Max-Planck Gesellschaft and Grant No. 321/4003/0318909A from the Bundesministerium für Forschung und Technologie (G.M.C. and A.M.G.), by the Medical Research Council of Canada grant to the Group of Protein Structure and Function at the University of Alberta (C.A.M. and M.N.G.J.), and by the Alberta Heritage Foundation for Medical Research (C.A.M.)

References

Bode,W., Papamakos,E., Musil,D., Seemueller,U. and Fritz,H. (1986) *EMBO J.*, **5**, 813–818.

Brooks,B.R., Bruccoleri,R.E., Olafson,B.D., States,D.J., Swaminathan,S. and Karplus,M. (1983) *J. Comput. Chem.*, **4**, 187–217.

Brünger,A.T., Clore,G.M., Gronenborn,A.M. and Karplus,M. (1986) *Proc. Natl. Acad. Sci. USA*, **83**, 3801–3805.

Clore,G.M., Nilges,M., Sukumaran,D.K., Brünger,A.T., Karplus,M. and Gronenborn,A.M. (1986a) *EMBO J.*, **5**, 2729–2735.

Clore,G.M., Brünger,A.T., Karplus,M. and Gronenborn,A.M. (1986b) *J. Mol. Biol.*, **191**, 523–551.

Clore,G.M., Gronenborn,A.M., Kjaer,M. and Poulsen,F.M. (1987a) *Protein Engineering*, **1**, 305–311.

Clore,G.M., Nilges,M., Brünger,A.T. Karplus,M. and Gronenborn,A.M. (1987b) *FEBS Lett.*, **213**, 269–277.

Kjaer,M. and Poulsen,F.M. (1987) *Carlsberg Res. Commun.*, in press.

McPhalen,C.A. and James,M.N.G. (1987) *Biochemistry*, **26**, 261–269.

McPhalen,C.A., Svendsen,I., Jonassen,I. and James,M.N.G. (1985a) *Proc. Natl. Acad. Sci. USA*, **82**, 7242–7246.

McPhalen,C.A., Schnebli,H.P. and James,M.N.G. (1985b) *FEBS Lett.*, **188**, 55–58.

Received on June 24, 1987